Natural and H2SO4 modified plane sawdust as a low-cost adsorbent: removal of anionic and cationic dyes from aqueous solutions

Duygu Ozdes[1] iD, Celal Duran[2]* iD, Sengul Tugba Ozeken[2] iD, Ozgun Kalkisim[3] iD, Yener Top[1] iD

[1] Gümüşhane University, Gümüşhane Vocational School, 29100, Gümüşhane, Türkiye
[2] Karadeniz Technical University, Faculty of Sciences, Department of Chemistry, 61080, Trabzon, Türkiye
[3] Recep Tayyip Erdoğan University, Faculty of Agriculture, Department of Horticulture, 53100, Rize, Türkiye

Abstract

Natural and H2SO4-modified plane (*Platanus orientalis* L.) sawdust were used for the adsorptive removal of cationic methylene blue (MB) and anionic indigo carmine (IC) dyes from aqueous media to suggest a new and cost-effective method for wastewater treatment applications. The influences of initial pH values, concentrations of MB and IC, period of contact, dosages of the natural and modified plane sawdust, and the presence of foreign ions on the adsorption of dyes were investigated in the experimental studies to describe the best conditions of the most efficient adsorption processes. Initial pH values were optimized to be between 6.0–8.0 for MB and 2.0 for IC. Optimum contact time to reach the equilibrium were determined as 120 and 240 min for the adsorption of MB onto NPS and MPS, respectively while IC adsorption onto both adsorbents reached the equilibrium in 240 min. By using the Langmuir isotherm model maximum MB adsorption capacities of NPS and MPS were calculated as 55.56 and 38.46 mg/g, respectively and the maximum IC adsorption capacities were 58.82 and 55.55 mg/g for NPS and MPS, respectively. Results showed that the natural and H2SO4-modified plane sawdust serve as low-cost and efficient materials in the adsorptive removal of MB and IC dyes for industrial wastewater treatment applications.

1. Introduction

The positive acceleration in technological development and the rapid increase in the world population led to the emergence of the problem of environmental pollution, which threatens human life and nature. Industrial dyestuffs, among the pollutants of organic origin, which exist in the wastewater of most industries release to the environment majorly from the textile, painting, leather, food, plastic, coating, and paper industries [1,2].

The complex organic structures of dyes make it time-consuming and difficult to remove them from industrial wastewater. Various techniques such as coagulation [3], flocculation [4], membrane filtration [5], photocatalytic degradation [6] and adsorption [2] are used to remove dyes from wastewater. Among these techniques, adsorption is one of the most-effective and low-capital investment-requiring methods. The adsorption method is based on the principle that solid substances called adsorbents retain the pollutants from the aqueous solutions by chemical or physical bonding [7]. In recent years, various adsorbents such as activated carbon, natural minerals, graphene oxide, and metal-organic frameworks used in dye removal are economically valuable materials [8]. Activated carbon is a popular adsorbent with a high adsorption capacity, used to remove many organic and inorganic pollutants from aqueous or gaseous media. However, the fact that commercial activated carbon is quite expensive makes the quest for low-cost adsorbents for the adsorption processes. For this reason, wood sawdust, which is cheap, effective, and modifiable in different ways to increase its capacity, is considered an adsorbent alternative to activated carbon. Such wastes are lignocellulosic materials containing three main structural components: hemicellulose, cellulose, and lignin. Sawdust attracts more interest from environmentalists since these materials are eco-friendly, abundant, accessible, cheap, and easily applicable in wastewater treatment. Pine, oak, fir, and hornbeam sawdust modified with cetyl trimethyl ammonium bromide (CTAB) [9], orange wood sawdust modified by

*Author of correspondence: cduran@ktu.edu.tr
Tel: +90 462 377 42 41
Fax: +90 462 325 31 96

sodium hydroxide (NaOH) [10], sugarcane pulp modified with formaldehyde [11], kail (*Pinus wallichiana*) sawdust [12], camphor (*Cinnamomum camphora*) sawdust [13], red pine sawdust [14], acacia sawdust [15], and many other types of sawdust wasted by the forest and agriculture industries that have no economic value, are found in the literature examining the potential of removing various dyes from aqueous solutions.

This study aimed to remove cationic methylene blue (MB) and anionic indigo carmine (IC) dyes from aqueous media through an adsorption process, using natural and H_2SO_4-modified plane sawdust as adsorbent materials. According to our literature research, although there are many studies [3,16] on MB removal from water since it is a widely used industrial dye and a model dye, there are limited studies on IC removal, which is also widely used. In the literature, there are studies in which different types of H_2SO_4-modified wastes are used for pollutant removal. Mahmood-ul-Hassan et al have used H_2SO_4-modified banana stalks, corn cob, and sunflower achene for the adsorption of Cd(II), Cr(III) and Pb(II) ions [17]. Mohebali et al have modified celery residue with H_2SO_4 to use as a low-cost adsorbent for elimination of MB from aqueous solution in batch adsorption process [18]. Djama et al have treated *Acorus calamus* firstly with H_2SO_4 and then activated by $KMnO_4$ to prepare an adsorbent for MB removal [19]. Zeydouni et al have used H_2SO_4-modified Aloe vera leaf shells for the removal of *P*-chlorophenol and MB from aqueous environment [20]. On the other hand, H_2SO_4-modified plane sawdust was used as an adsorbent for the first time in the adsorption of MB and IC in the present study. There are various modification agents to improve the adsorptive specifications of an adsorbent in the literature, yet H_2SO_4 was preferred as a chemical agent to modify the natural plane sawdust material due to the advantages of being inexpensive and simply applicable [21]. In order to obtain the optimum retention conditions, the influences of significant experimental parameters, including initial solution pH, initial dye and adsorbent concentration, and contact time on the process were evaluated. The adsorption isotherms were utilized to calculate the MB and IC adsorption capacity of NPS and MPS and to interpret the adsorption mechanism.

2. Materials and Method

2.1. Preparation of natural and modified adsorbents
Natural plane sawdust was ground without any physical or chemical pretreatments and sifted to obtain particles smaller than 150 μm for the experiments. To obtain H_2SO_4-modified plane sawdust, 20 g of plane sawdust was stirred well with 20 mL of concentrated H_2SO_4 on a hot plate at 200°C for 24 hours, and then washed with distilled water to remove acidic residues. After washing, the sample was soaked in aqueous $NaHCO_3$ at 1% (w/v) concentration for 24 hours to neutralize the acidic residues, then washed with distilled water and dried in the oven at 105°C for 24 hours [21] and ground and sifted to separate the particles smaller than 150 μm for the experimental studies.

2.2. Chemicals and apparatus
Methylene blue ($C_{16}H_{18}ClN_3S$), indigo carmine ($C_{16}H_8N_2Na_2O_8S_2$), H_2SO_4, HNO_3, NaOH, $NaHCO_3$, Na_2CO_3, and HCl were analytical grade chemicals used in this study and purchased from Fluka (Buch, Switzerland) and Merck (Darmstadt, Germany) companies. Distilled water was used in all experimental stages. Perkin Elmer 1600 FT-IR model spectrophotometer was utilized for the FTIR analysis of the surface functional groups. Santen SE 125 model furnace was used for moisture analysis. Perkin Elmer Lambda 25 model UV-Vis spectrophotometer was used to determine the concentration of dyes remaining in the aqueous solutions. BOECO PSU-15i model mechanical shaker was used for shaking the samples in the adsorption stage. BOECO S-8 model centrifuge device was used to separate the solid and liquid phases from each other. Hanna pH-2221 model desktop digital pH meter was used to adjust the initial pH of the dye solutions. All samples were weighed by Sartorius BP1106 model analytical balance and stirred by IKA RCT Basic model magnetic stirrer.

2.3. Batch experiments
Adsorption experiments were utilized through the batch method in polypropylene centrifuge tubes. The initial pH of the MB and IC solutions was adjusted by diluted HNO_3 or NaOH solutions. Ten milliliters of MB or IC in the concentration range between 50 and 1000 mg/L was added to each sample of adsorbent (NPS or MPS) weighed (0.01–0.20 g) in the centrifuge tubes, and the samples were shaken on a mechanical shaker at 350 rpm for various contact times ranging between 1–360 min. After the adsorption process, the solid and liquid phases were separated from each other in the stage of centrifuging at 3500 rpm for 5 min, and the remaining concentrations of dyes in the supernatant solutions were measured by a UV-Vis spectrophotometer at 663 and 609 nm wavelengths for MB and IC, respectively. The amounts of adsorbed MB or IC dyes onto 1 g of NPS or MPS adsorbent (mg/g) and the percentage of adsorption (%) were calculated by using Eq.1 and Eq.2, respectively.

$$q_e = \frac{(C_o - C_e) \times V}{m} \qquad (1)$$

$$Adsorption \ (\%) = \frac{C_o - C_e}{C_o} \times 100 \qquad (2)$$

q_e (mg/g) is the amount of adsorbed dye onto 1 g of NPS or MPS, C_o (mg/L) is the initial concentration of MB or IC, C_e (mg/L) is the concentration of the unadsorbed MB or IC at the equilibrium, V (L) is the volume of the dye solution, and m (g) is the dry mass of the NPS or MPS.

3. Results and Discussion

3.1. Characterization of NPS and MPS
Characterizations of NPS and MPS were evaluated by FTIR, moisture content and pH_{pzc} analysis, and Boehm titration method. Functional groups on the surface of NPS and MPS were determined by FTIR analysis, as represented in Fig. 1 (a) and (b), respectively. Most of the functional groups on NPS were kept the same in the modified adsorbent since the modification process was utilized in low temperatures. The broad peak at 3396 cm^{-1} can be attributed to –OH groups of phenolic, carboxylic, and alcoholic groups in the samples. The peak in 1454 cm^{-1} also corresponds to phenolic –OH groups. The peaks at 2918, 2852 and 1372 cm^{-1} are the aliphatic C–H bonds. The peak at 1734 cm^{-1} corresponds to the C=O stretching of the carbonyl groups. The peak at 1051 cm^{-1} is a sign of the C–C bond, and the peaks between 1051–1237 cm^{-1} point out the presence of S=O groups in the structure. The peaks at 1646 and 1051 cm^{-1} are the stretching peaks of C=C and C–O bonds, and the peak at 892 cm^{-1} makes a sign to C–O–H groups [22–24].

The amounts of lactonic, phenolic, and carboxylic groups on the surface of natural and modified plane sawdust were determined by the Boehm titration method [25].
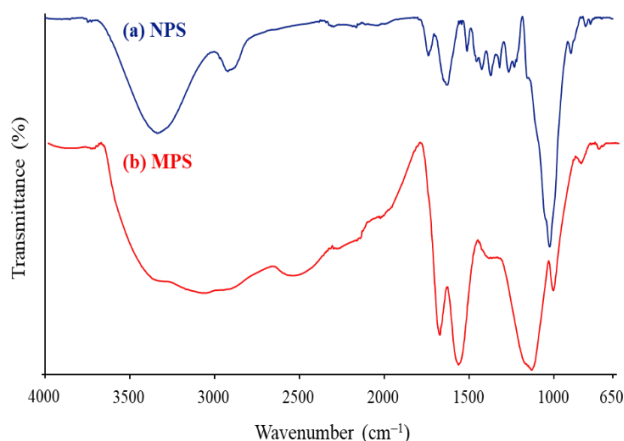

Figure 1. FTIR spectra of a) NPS and b) MPS

Table 1. Some characterization parameters of the adsorbents

Parameters	NPS	MPS
pH_{pzc}	4.6	–
Moisture content (%)	6.87	10.93
Surface acidic groups (mmol/g)		
Lactonic groups	1.23	2.14
Carboxylic groups	4.28	11.78
Phenolic groups	1.22	5.66
Total acidic groups (mmol/g)	6.73	19.58

Quantitative data of carboxylic, phenolic, and lactonic groups showed that surfaces of the adsorbents were rich in total acidic groups that increased by the modification process, especially the number of carboxylic groups increased the most (Table 1). As the temperature of the modification process, which increases the adsorption capacity and plays a significant role in the adsorptive removal of pollutants from aqueous solutions, is limited in the range of 200–400°C, high numbers of acidic oxides were obtained on the surface of the activated adsorbent [26].

3.2. Effect of pH on the adsorption process
The effect of the initial pH of the dye solutions in contact with each adsorbent was the first parameter studied for the best selection of the appropriate adsorbate-adsorbent systems since the initial pH directly affects the adsorption efficiency. MB and IC concentrations were 50 mg/L in separate solutions. MB solutions with a natural pH of 6.5 and adjusted pH values in the range of 2.0–8.0 and IC solutions with a natural pH and adjusted pH values in the range of 1.0–8.0 were tested for the optimization of the initial pH. Diluted HNO$_3$ and NaOH were used to adjust the pH of dye solutions. The NPS or MPS (5.0 g/L) was shaken with the dye solutions at various initial pH values on the mechanical shaker for 240 min and centrifuged at 3500 rpm for 5 min to separate the solid and the liquid phases. The concentrations of the remaining dyes in the supernatants were analyzed by the UV-Vis spectrophotometer.

As seen in Fig. 2 (a), the adsorption efficiency of the adsorbents performed best in the pH range of 6.0–8.0 in the adsorption of cationic MB dye. However, the adsorption efficiency in the MB adsorption onto NPS and MPS reached a value higher than 90% at pH 6.5 which corresponds to the natural (unadjusted) pH of the MB solution. The adsorption efficiencies of the MPS reached a value higher than 95% in the pH range of 2.0–8.0, also pointing out that not the electrostatic attractions only but also an ion-exchange-based mechanism may be possible to explain the adsorption process. In the adsorption of MB dye, natural adsorbent performed low adsorption efficiency, which increased by the increase in solution pH. On the other hand, the adsorption

efficiency reached its maximum value at pH 2.0 in the adsorption of IC dye, as seen in Fig. 2 (b). In the pH range of 1.0–2.0, the efficiencies of IC adsorption onto NPS and MPS are higher than 90%, yet the adsorption efficiencies decreased immediately as the initial pH of dye solutions increased.

The adsorption efficiencies are low in MB adsorption and high in IC adsorption in acidic initial pH values since the environments of the NPS and MPS are surrounded by H_3O^+ ions, and the functional groups of the solid adsorbents electrically charged positively in the acidic aqueous media. The electrostatic repulsion between the H_3O^+ ions and the cationic MB dye prevents the approaching of the adsorbent and the adsorbate. As the initial pH of the solution increases, the adsorption efficiency increases due to decreasing competitive adsorption behavior of H_3O^+ ions and cationic MB dye onto active sites. However, anionic IC dye approaches the positively charged surface of the adsorbent due to electrostatic attractions in low initial pH values. As the initial pH of the solution increases, the adsorption efficiency decreases due to the increased competitive adsorption behavior of OH^- ions and anionic IC dye onto active sites [27,28].

The pH_{pzc} value was found to be 4.6 for NPS, revealing that the number of acidic functional groups is higher than the basic functional groups in its chemical structure. Informative numerical data about the pH_{pzc} value of an adsorbent is essential to optimize the initial pH to reach the highest adsorption efficiency since the net surface charge of the adsorbent is positive if pH < pH_{pzc} and negative if pH > pH_{pzc} [29]. The cationic dyes are adsorbed better at pH values higher than pH_{pzc}, and the anionic dyes are adsorbed better at lower pH values than pH_{pzc} [30]. As a result, further experiments were planned through the optimized initial pH values of 6.5 for MB and 2.0 for IC adsorption.

3.3. Effect of contact time on the retention of MB and IC
Optimization of the contact time was evaluated by testing various periods of contact. Ten milliliters of MB solution with a natural pH of 6.5 or IC solution with an adjusted pH of 2.0 was added onto 5.0 g/L of NPS or MPS, which were weighed in polypropylene centrifuge tubes and processed for adsorption on the mechanical shaker for various periods ranging between 1–360 min. After shaking, the samples were centrifuged to separate the solution and the adsorbent from each other. The concentration of each dye remaining in the solution was determined by UV-Vis Spectrophotometer and used to calculate the amount of MB or IC dyes adsorbed onto 1 g of adsorbent (q_t) for different contact times.
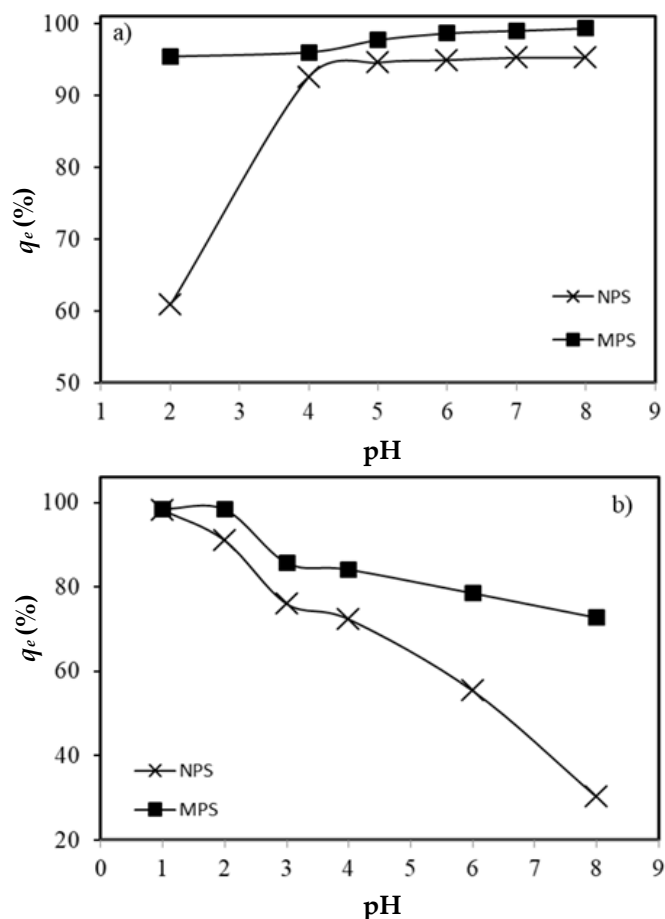

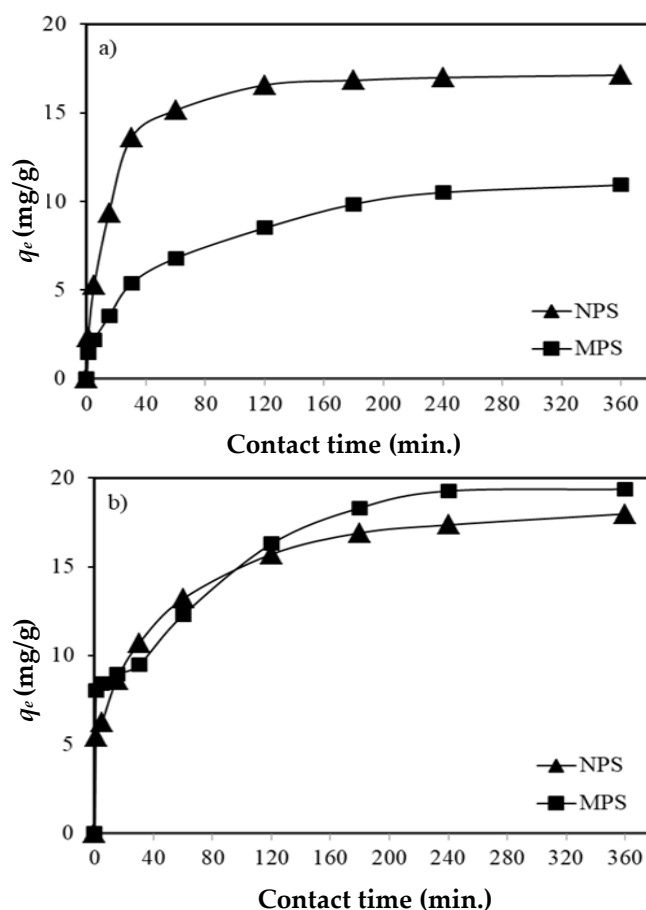Figure 2. Impact of initial pH on a) MB and b) IC uptake onto NPS and MPS

Figure 3. Influences of contact time on a) MB and b) IC uptake onto NPS and MPS

In the adsorption of MB onto NPS and MPS, optimum contact times to reach the equilibrium were determined to be 120 and 240 min, respectively (Fig. 3 (a)), while the process of IC adsorption onto NPS and MPS reached the equilibrium in 240 min (Fig. 3 (b)). The amount of adsorbed MB and IC onto all adsorbents became nearly stable after reaching the equilibrium. The dye sorption process occurs immediately in the first stages since the active sites of NPS and MPS surfaces were available for adsorption. The transportation of the dye molecules into the internal surfaces of the pores through diffusion slows down when the system becomes closer to equilibrium. After reaching the equilibrium, the amounts of adsorbed dye do not increase much according to the saturation of the adsorptive sites [31]. As a result, the equilibration time for both dyes was determined as 240 min in subsequent studies to ensure that the equilibrium was fully established.

3.4. Effect of initial dye concentration and isotherm studies

The solutions of MB and IC at various initial concentrations in the range of 50–1000 mg/L were added onto 5.0 g/L of NPS and MPS adsorbents separately to determine the effect of initial dye concentration on the adsorption process. Then the mixtures were shaken on the mechanical shaker at 350 rpm for 240 min to reach the equilibrium. After centrifuging the samples, the amount of unadsorbed MB or IC remaining in the supernatant was analyzed by UV-Vis spectrophotometer. The initial concentration of MB was plotted against the adsorbed amounts (q_e) and the removal percentage (%) of MB onto NPS and MPS (Fig. 4 (a,b), and the same parameters were plotted for the data obtained in IC's adsorption onto NPS and MPS as demonstrated in Fig. 4 (c,d). Increased initial concentrations of the dye resulted in increased amounts of MB or IC adsorbed per g of the adsorbent due to the occurring concentration gradient that improves the adsorption. On the other hand, the percentages of adsorption decreased at high initial dye concentrations because of the oversaturation of the active adsorption sites of the sorbents' surface [32].

The Langmuir, Freundlich, and Dubinin-Radushkevich isotherm models were fitted to the experimental data to get an idea of the surface structure of NPS and MPS and to interpret the MB and IC adsorption mechanism. According to the Langmuir isotherm model, the adsorbent has a homogenous surface consisting of a constant number of co-energized active sites, and there are no interactions between the adsorbate molecules [33]. Eq.3 and Eq.4 are the non-linear and linear forms of the Langmuir isotherm model.
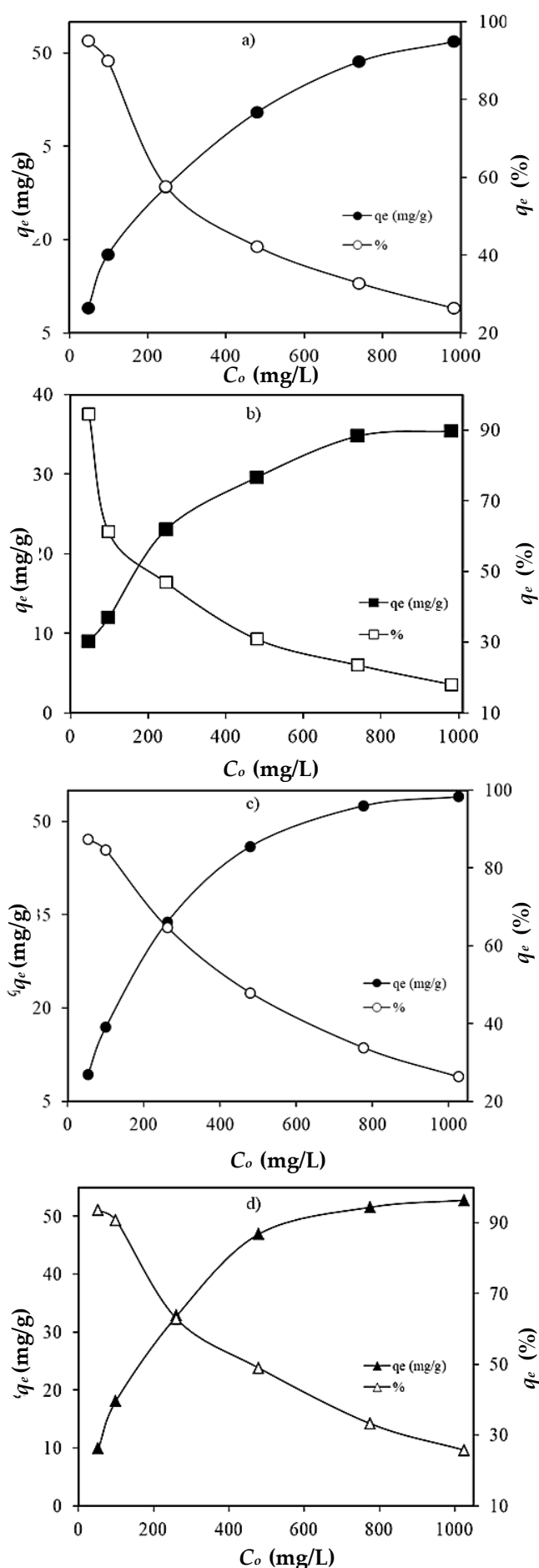
$$q_e = \frac{bC_e}{1 + bC_e} \qquad (3)$$

Figure 4. Effect of initial dye concentration on the adsorption of a) MB onto NPS b) MB onto MPS c) IC onto NPS d) IC onto MPS

$$\frac{C_e}{q_e} = \frac{C_e}{q_{max}} + \frac{1}{bq_{max}} \qquad (4)$$

q_e (mg/g) is the adsorbed amount of adsorbate onto 1 g of adsorbent, q_{max} (mg/g) is the adsorption capacity, C_e (mg/L) is the concentration of the remaining adsorbate in the solution at the equilibrium, and b (L/mg) is a constant related to the free energy. The slope and the intercept of the C_e/q_e vs. C_e plot are used to determine q_{max} and b.

Dimensionless R_L constant calculated by Eq.5 [34] gives an idea about the favorability of the adsorption process for an adsorbate-adsorbent pair.

$$R_L = \frac{1}{1 + bC_o} \qquad (5)$$

C_o (mg/L) is the initial concentration of the adsorbate in the solution, and b (L/mg) is the Langmuir constant. There are four possible values of R_L which are evaluated to four possible definitions as the adsorption process is,

i.   Favorable in the experimental conditions if $0 < R_L < 1$,
ii.   Irreversible if $R_L = 0$,
iii. Linear if $R_L = 1$, and
iv.   Unfavorable if $R_L > 1$.

The adsorptive sites on the surface of the adsorbent are accepted to be consisting of different types of sites and regions settled heterogeneously and energized variously in the Freundlich isotherm model as described in Eq. 6 [35] and linearizes to Eq. 7 by evaluating through the function of logarithms.

$$q_e = K_f \times C_e^{1/n} \qquad (6)$$

$$ln(q_e) = ln(K_f) + \frac{1}{n}ln(C_e) \qquad (7)$$

q_e (mg/g) is the amount of the adsorbed adsorbate onto 1 g of adsorbent, K_f (mg/g) is the adsorption capacity, C_e (mg/L) is the amount of unadsorbed adsorbate remaining in the solution at the equilibrium, and n is the density of adsorption. K_f and n are the constants obtained from the intercept and slope of the plot of $ln(q_e)$ vs. $ln(C_e)$, respectively. The heterogeneity factor (n) ranging between 1 and 10 is a sign of the favorability of the adsorption system [36].

Dubinin–Radushkevich (D–R) isotherm model (Eq. 8) explains the adsorption onto similarly porous surface structures [37], and this model reminds the Langmuir model in this respect.

$$ln(q_e) = ln(q_m) - K\varepsilon^2 \qquad (8)$$

q_e (mol/g) is the adsorbed amount of the adsorbate per g of adsorbent, q_m (mol/g) is the monolayer adsorption capacity, and K (mol²/kJ²) is the constant of adsorption energy. ε is Polanyi potential which is calculated by Eq. 9.

$$\varepsilon = RTln(1 + 1/C_e) \qquad (9)$$

R (J/mol/K) is the gas constant, C_e (mol/L) is the concentration of the unadsorbed adsorbate remaining in the solution at the equilibrium, and T (K) is the temperature. K and q_m values are obtained from the slope and intercept of the ε^2 vs. $ln\ q_e$ plot, respectively. K values obtained by the D–R isotherm are evaluated in Eq. 10 to calculate E (kJ/mol).

$$E = 1/(-2K)^{1/2} \qquad (10)$$

The average adsorption energy (E) gives information about the chemical and physical specifications of the adsorption. There are three possibilities about the value of E evaluated as the adsorption occurs,

i.   Physically if $E < 8$ kJ/mol,
ii.   Through ion-exchange if $8 < E < 16$ kJ/mol, and
iii. Chemically if $E > 16$ kJ/mol [38].

Experimental data was applied to Langmuir, Freundlich, and D–R isotherm models to explain the mechanisms of MB and IC adsorption onto NPS and MPS. The non-linear equations of these three models were evaluated to obtain the isotherm plots (C_e vs. q_e) for MB adsorption onto NPS and MPS (Fig.5 (a,b)) and IC adsorption onto NPS and MPS (Fig.5 (c,d), respectively.

q_{max} and b are the Langmuir constants which were determined by the slope and the intercept of the C_e vs. C_e/q_e plot, respectively, while n and K_f are the constants of Freundlich isotherm, which were determined by the slope and the intercept of the $ln(C_e)$ vs. $ln(q_e)$ plot. The results of the calculations on the experimental data for MB and IC adsorption onto NPS and MPS were tabulated with the correlation coefficients (R^2) in Table 2.

The R^2 values obtained by the application of the Langmuir model were higher than those for the Freundlich model for both dyes, indicating that the active adsorption sites on the surfaces of NPS and MPS were distributed homogeneously [39]. Maximum MB adsorption capacities of NPS and MPS calculated as 55.56 and 38.46 mg/g by the Langmuir isotherm model, respectively, were compared to other adsorption studies in the literature.

Table 2. Isotherm model parameters

| Langmuir isotherm model	NPS-MB	MPS-MB	NPS-IC	MPS-IC
q_{max} (mg/g)	55.56	38.46	58.82	55.55
b (L/mg)	0.020	0.016	0.021	0.029
R^2	0.985	0.990	0.998	0.996
Freundlich isotherm model				
K_f (mg/g)	7.71	6.12	5.54	7.93
n	3.41	3.82	2.74	3.31
R^2	0.983	0.936	0.959	0.968
D–R isotherm model				
q_m (mg/g)	9.62	7.49	11.94	10.60
K (kJ²/mol²)	-0.002	-0.002	-0.003	-0.002
E (kJ/mol)	12.91	12.91	12.91	15.81
R^2	0.986	0.899	0.980	0.983

On the other hand, the maximum IC adsorption capacities were 58.82 and 55.55 mg/g for NPS and MPS adsorbents, yet there have not found enough studies about the adsorption of IC in the literature to compare with the results of this study. The adsorption capacities of NPS and MPS are higher than many adsorbents, which were expensive or not easily prepared, as seen in the table of comparison (Table 3) [29,40–49].

As the maximum adsorption capacities of natural and H_2SO_4-modified plane sawdust compared to each other, NPS performed better than MPS in MB adsorption, while there was no meaningful difference between the natural and modified adsorbents in IC adsorption. Closer adsorption capacities of natural and H_2SO_4-modified adsorbents in IC adsorption can be explained by the fact that although the surface areas of the modified adsorbents partially increased by the low-temperature modification process, the resulting sulfate salts may have clogged the pores.

As seen in Table 2, the constants of the D–R isotherm model were determined by the evaluation of the slope

Table 3. Comparison of the dye uptake capacities of the different sorbents from literature

Adsorbent	Adsorbate	q_{max} (mg/g)	Ref.
Celery residue modified with H_2SO_4 was	MB	476.19	[18]
Acorus calamus treated with H_2SO_4 and activated by $KMnO_4$	MB	1500	[19]
H_2SO_4-modified Aloe vera leaf shells	MB	192.3	[20]
Microwave assisted sawdust	MB	58.14	[29]
Canola residues	MB	13.22	[40]
Carbon nanotubes	MB	46.20	[41]
Titanium dioxide nanotube	MB	57.14	[42]
Magnetic $ZnO/ZnFe_2O_4$	MB	37.27	[43]
Peanut hull	MB	68.03	[44]
Activated carbons from sunflower oil cake modified by H_2SO_4	MB	16.43	[45]
Tartaric acid modified wheat bran	MB	25.18	[46]
Biochar derived from eucalyptus saw dust modified with acetic acid	MB	29.94	[47]
Orange peel	MB	13.90	[48]
Banana peel	MB	20.80	[48]
Original beech sawdust	MB	9.78	[49]
$CaCl_2$ treated beech sawdust	MB	13.02	[49]
Natural plane sawdust	MB and IC	55.56 and 58.82	This study
H_2SO_4-modified plane sawdust	MB and IC	38.46 and 55.55	This study
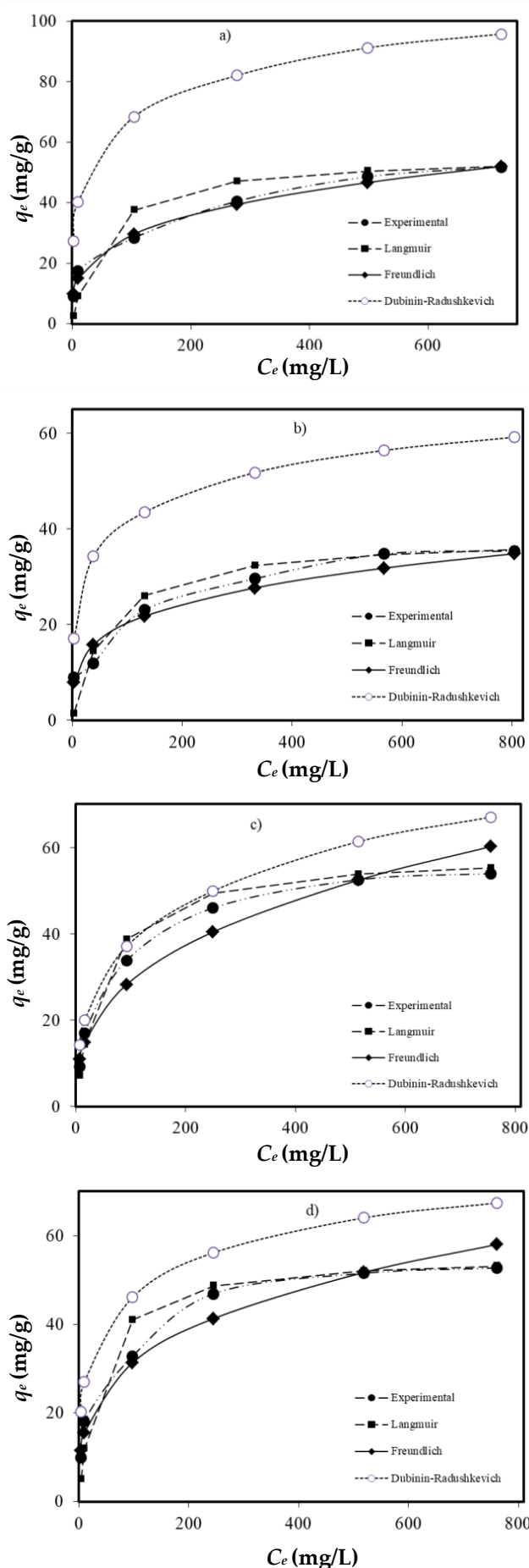
Figure 5. Adsorption isotherms of a) MB adsorption onto NPS a) MB adsorption onto NPS a) IC adsorption onto NPS a) IC adsorption onto NPS

and the intercept of the ε^2 versus $\ln q_e$ plot as the values of K and q_m, respectively. E is the mean energy of the adsorption calculated from the value of K. E values were in the range of 8–16 kJ/mol in all calculations suggesting that ion-exchange mechanisms were also effective in the adsorption of MB and IC onto NPS and MPS [38].

R_L values were calculated to figure out the suitability of adsorption onto NPS and MPS and found to be in the range of 0–1, while the initial concentrations of MB and IC were between 50–1000 mg/L. As the initial dye concentration of the dye increased, the R_L values decreased in the range of $0 < R_L < 1$, suggesting that the processes in both dyes' adsorption onto the natural and H2SO4-modified plane adsorbents were favorable in the relevant experimental conditions. Additionally, n values obtained by the Freundlich isotherm model were in the 1–10 range, supporting the idea that MB and IC adsorption onto NPS and MPS were favorable.

3.5. Effect of adsorbent dosage on the adsorption efficiency

The suspensions consisting of 0.01–0.20 g (1.0–20.0 g/L) of NPS or MPS adsorbent and 200 mg/L MB or IC solutions were processed for 240 min on the mechanical shaker to investigate the effect of adsorbent dosage on the adsorption efficiency. After reaching the equilibrium, the concentrations of unadsorbed MB and IC remaining in the supernatants were determined by using a UV-Vis spectrophotometer. The adsorbed amounts (q_e) and removal percentages (%) of MB onto NPS and MPS were plotted against the amounts of NPS and MPS in Fig. 6 (a,b), and the adsorbed amounts (q_e) and removal percentages (%) of IC dyes against the amounts of NPS and MPS adsorbents were plotted as represented in Fig. 6 (c,d), respectively.

Increasing the amounts of NPS and MPS increased the unsaturated surfaces at the constant concentrations of MB and IC and decreased the amounts of adsorbed dye onto 1 gram of each adsorbent (q_e) due to the decreased surface area caused by a possible aggregation. However, increasing the dosage of NPS and MPS resulted in increased removal percentages caused by the number of active sites becoming higher in number [50].

3.6. Effect of foreign ions on the adsorption efficiency

Dye-contaminated wastewater sourced by textile industries may include high amounts of foreign ions, which cause ionic strength and decrease the adsorption efficiency. NaCl and BaCl2 solutions in various concentrations between 0.05–0.5 M were separately added to 100 mg/L MB and IC solutions and processed to investigate the effect of salts on the adsorption efficiency.
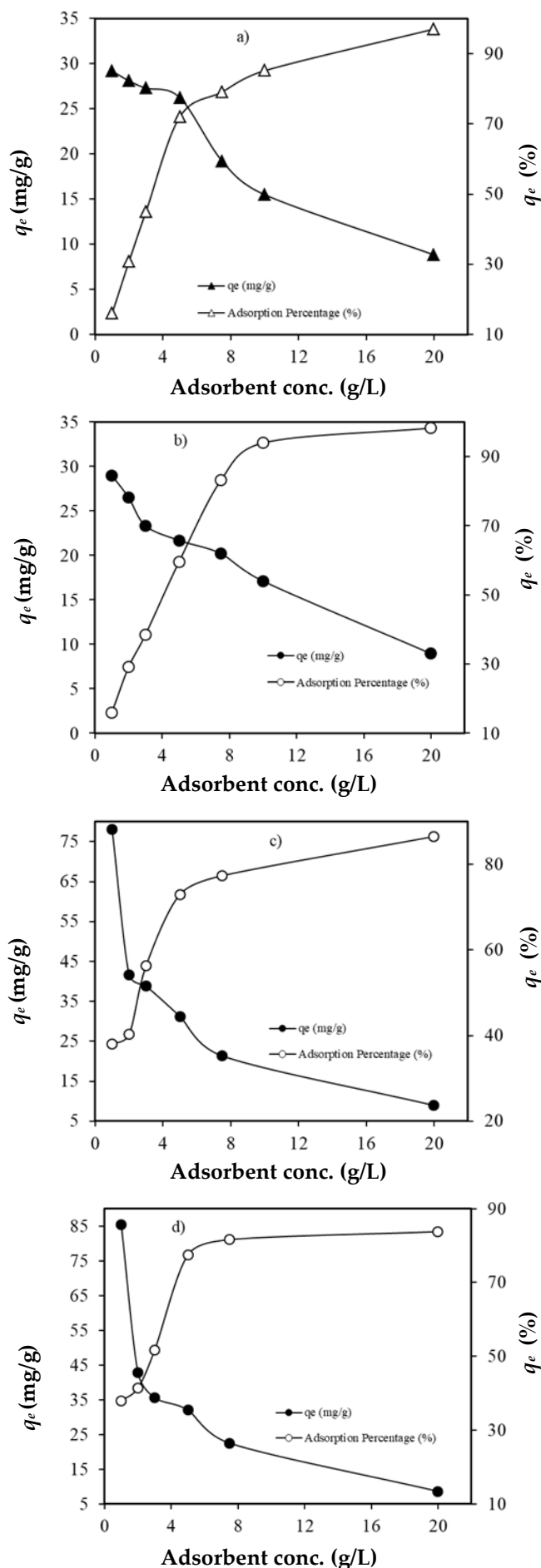

Figure 6. Effect of adsorbent amount on the adsorption of a) MB onto NPS b) MB onto MPS c) IC onto NPS d) IC onto MPS

The presence of salts may result in two effects opposite to each other. The first one is the prevention of the electrostatic interactions between the dye molecules and the active adsorption sites as the salt concentration increases, which decreases the adsorbed amounts of dye. This effect is observed in the adsorption of MB onto NPS and MPS (Fig. 7 (a,b)). The presence of both salts (NaCl and BaCl2) in the solution prevents the attachment of MB molecules onto the active adsorptive sites of the adsorbent's surface, and the adsorption efficiency decreases when the salt concentration increases [51]. The other effect is an increase in the dissociation of dye molecules caused by ionic strength. The amount of adsorbed dye increases when the ionic strength increases since the dissociated dye molecules become free to bind onto the surface electrostatically, as observed in IC adsorption onto NPS and MPS (Fig. 7 (c,d)). Increased concentrations of NaCl and BaCl2 caused increased adsorption according to the increased dissociation degree of IC [52].

4. Conclusion

In this study, the adsorption behaviors of natural and H2SO4-modified sawdust of plane (*Platanus orientalis* L.) were investigated for the adsorptive removal of pollutant methylene blue and indigo carmine dyes from aqueous media to suggest a new method for the treatment of dye contaminated industrial wastewater. Natural and H2SO4-modified adsorbents were characterized via FT–IR Spectroscopy, pH_{pzc} and moisture content analysis, and the Boehm titration method. The optimum pH values at which the highest adsorption efficiencies were performed were determined as 6.0–8.0 range for cationic MB dye and 2.0 for anionic IC dye's adsorption onto NPS and MPS. The adsorption process reached the equilibrium in 240 min in IC adsorption onto NPS and MPS. On the other hand, the process reached equilibrium in 120 and 240 min in MB adsorption onto NPS and MPS, respectively. Both dyes were tested for all other parameters for 240 min of contact time. The amounts of adsorbed MB and IC per gram of any adsorbent decreased, and the percentage of adsorption increased with the increasing initial concentrations of both dyes. The adsorption of MB and IC fit well with the Langmuir isotherm model, suggesting that the surfaces of NPS and MPS consisted of homogeneous active sites in nature. The Langmuir maximum monolayer adsorption capacities of NPS and MPS adsorbents were higher than many expensive and hardly prepared adsorbents reported before. The information of decreasing R_L values in the 0–1 range while the concentrations of MB and IC dyes were increasing was supported by all the n values
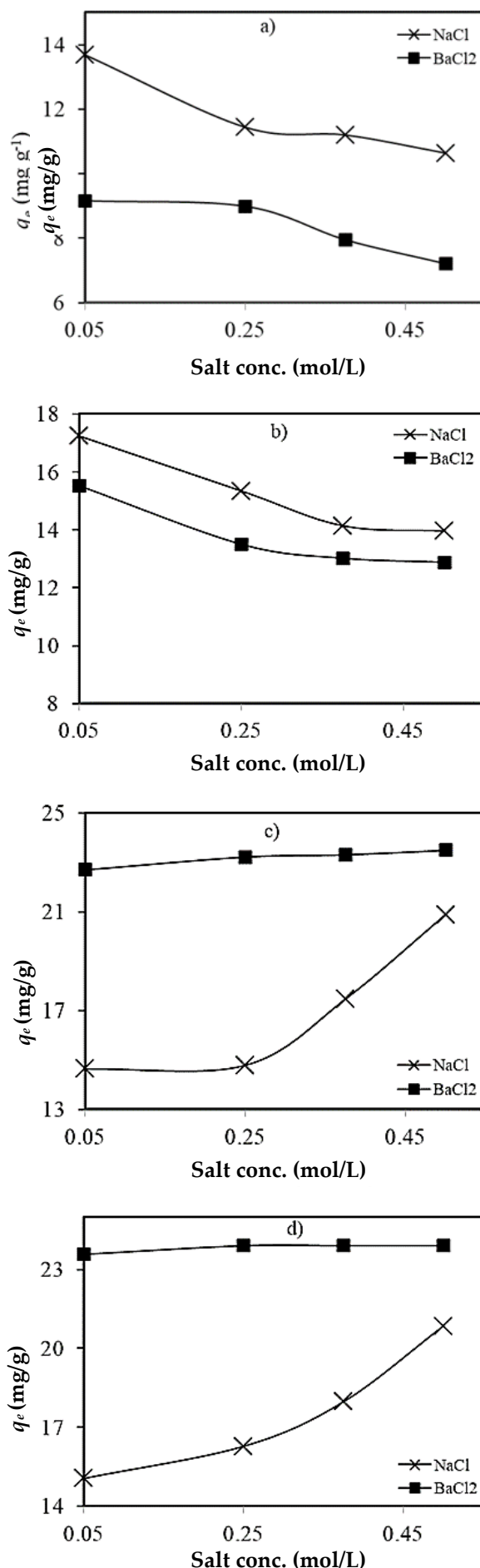

Figure 7. Effect of salt concentration on the adsorption of a) MB onto NPS b) MB onto MPS c) IC onto NPS d) IC onto MPS

corresponding to the range of 1–10 obtained from the Freundlich isotherm model, and these results indicated that the adsorption of both dyes onto NPS and MPS were favorable processes in this study. The adsorption efficiency decreased in MB adsorption and increased in IC adsorption due to the ionic strength in the presence of foreign ions, which were introduced to the aqueous media by NaCl and BaCl$_2$ salts. Natural and H$_2$SO$_4$–modified plane sawdust can be used as low-cost and effective adsorbents for the adsorptive removal of MB and IC.

Funding

References

[1] B.I. Musah, L. Peng, Y. Xu, Adsorption of Methylene Blue Using Chemically Enhanced *Platanus orientalis* Leaf Powder: Kinetics and Mechanisms, Nat Environ Pollut Technol, 19, 2020, 29–40.

[2] M. Peydayesh, A. Rahbar-Kelishami, Adsorption of methylene blue onto Platanus orientalis leaf powder: Kinetic, equilibrium and thermodynamic studies, J Ind Eng Chem, 21, 2015, 1014–1019.

[3] D. Morshedi, Z. Mohammadi, M.M.A. Boojar, F. Aliakbari, Using protein nanofibrils to remove azo dyes from aqueous solution by the coagulation process, Colloids Surf B Biointerfaces, 112, 2013, 245-254.

[4] X. Xiao, Y. Sun, W. Sun, H. Wu, C. Liu, Advanced treatment of actual textile dye wastewater by Fenton-flocculation process, Can J Chem Eng, 95(7), 2017, 1245–1252.

[5] M.F. Abid, M.A. Zablouk, A.M. Abid-Alameer, Experimental study of dye removal from industrial wastewater by membrane technologies of reverse osmosis and nanofiltration, Iranian J Environ Health Sci Eng, 9,2012, 17.

[6] M. Koç Keşir, G. Dilber, M. Sökmen, M. Durmuş, Use of new quaternized water soluble zinc phthalocyanin derivatives for effective dye sensitization of TiO$_2$, J Solgel Sci Technol, 93, 2020, 687–694.

[7] N.A. El Essawy, S.M. Ali, H.A. Farag, M. Elnouby, H.A. Hamad, Green synthesis of graphene from recycled PET bottle wastes for use in the adsorption of dyes in aqueous solution, Ecotoxicol Environ Saf, 145, 2017, 57–68.

[8] A.A. Mohammadi, S. Moghanlo, M.S. Kazemi, S. Nazari, S.K. Ghadiri, H.N. Saleh, M. Sillanpää, Comparative removal of hazardous cationic dyes by MOF-5 and modified graphene oxide, Sci Rep, 12, 2022,15314.

[9] F. Deniz, R.A. Kepekci, Biosorption of Food Green 3 by a novel green generation composite biosorbent from aqueous environment, Int J Phytoremediation, 19(6), 2017, 579–586

[10] A.A. Azzaz, S. Jellali, H. Akrout, A.A. Assadi, L. Bousselmi, Optimization of a cationic dye removal by a chemically modified agriculture by-product using response surface methodology: biomasses characterization and adsorption properties, Environ Sci Pollut R, 24(11), 2017, 9831–9846.

[11] T. Aftab, F. Bashir, B. Khan, J. Iqbal, R.A. Khan, Equilibrium and kinetics of color adsorption on agriculture by-products/wastes (Sugarcane bagasse, corncob, sawdust), Desalin Water Treat, 65, 2017, 109–116.

[12] V. Gupta, A. Agarwal, M.K. Singh, N.B. Singh, Removal of torque blue dye from aqueous solution by Kail Sawdust, Asian J Water Environ Pollut, 13(4), 2016, 59–67.

[13] H. Wang, X. Yuan, Z. Wu, L. Leng, G. Zeng, Removal of Basic Dye from Aqueous Solution using *Cinnamomum camphora* Sawdust: Kinetics, Isotherms, Thermodynamics, and Mass-Transfer Processes, Sep Sci Technol, 49, 2014, 2689–2699.

[14] M. Can, Equilibrium, kinetics and process design of acid yellow 132 adsorption onto red pine sawdust, Water Sci Technol, 71(12), 2015, 1901–1911.

[15] M. Jain, A. Mudhoo, V.K. Garg, Swiss blue dye sequestration by adsorption using *Acacia nilotica* sawdust, Int J Env Technol Manag, 14(1–4), 2011, 220–237.

[16] F.A. Khan, A. Ahad, S.S. Shah, M. Farooqui, Adsorption of crystal violet dye using *Platanus orientalis* (Chinar tree) leaf powder and its biochar: equilibrium, kinetics and thermodynamics study, Int J Environ Analyt Chem, 2021, 1–21.

[17] M. Mahmood-ul-Hassan, V. Suthor, E. Rafique, M. Yasin, Removal of Cd, Cr, and Pb from aqueous solution by unmodified and modified agricultural wastes, Environ Monit Assess, 187, 2015, 19.

[18] S. Mohebali, D. Bastani, H. Shayesteh, Methylene blue removal using modified celery (*Apium graveolens*) as a low-cost biosorbent in batch mode: Kinetic, equilibrium, and thermodynamic studies, J Mol Struct, 1173, 2018, 541–551.

[19] C. Djama, D. Chebli, A. Bouguettoucha, I. Doudou, A. Amrane, Statistical physics modelling of azo dyes biosorption onto modified powder of *Acorus calamus* in batch reactor, Biomass Convers Biorefinery, 13, 2023, 1013–1028.

[20] G. Zeydouni, S. R. Couto, H. Nourmoradi, H. Basiri, P. Amoatey, S. Esmaeili, S. Saeidi, F. Keishams, M. J. Mohammadi, Y. O. Khaniabadi, H$_2$SO$_4$-modified *Aloe vera* leaf shells for the removal of *P*-chlorophenol and methylene blue from aqueous environment, Toxin Reviews, 39 (1), 2020, 57–67.

[21] C. Duran, D. Ozdes, A. Gundogdu, M. Imamoglu, H.B. Senturk, Tea-industry waste activated carbon, as a novel adsorbent, for separation, preconcentration and speciation of chromium, Anal Chim Acta, 688, 2011, 75–83.

[22] A.W. Adamson, Physical Chemistry of Surfaces (2nd Edition), 1967, New York: Interscience.

[23] J. Guo, A.C. Lua, Textural and Chemical Characterizations of Adsorbent Prepared from Palm Shell by Potassium Hydroxide Impregnation at Different Stages, J Colloid Interf Sci, 254, 2002, 227–233.

[24] I.A.W. Tan, A.L. Ahmad, B.H. Hameed, Preparation of Activated Carbon from Coconut Husk: Optimization Study on Removal of 2,4,6-Trichlorophenol Using Response Surface Methodology, J Hazard Mater, 153, 2008, 709–717.

[25] H.P. Boehm, Chemical Identification of Surface Groups, Adv Catal, 16, 1966, 179–274.

[26] J.S. Mattson, H.B. Mark, Jr, Activated Carbon, 1971, New York: Marcel Dekker.

[27] V.K. Garg, A. Moirangthem, R. Kumar, R. Gupta, Basic dye (methylene blue) removal from simulated waste water by adsorption using Indian Rosewood Sawdust: timber industry waste, Dyes Pigments, 63, 2004, 243–250.

[28] V.K. Gupta, R. Jain, S. Malathi, A. Nayak, Adsorption-desorption studies of indigocarmine from industrial effluents by using deoiled mustard and its comparison with charcoal, J Colloid Interf Sci, 348(2), 2010, 628-633.

[29] S. Suganya, P. Senthil Kumar, A. Saravanan, P. Sundar Rajan, C. Ravikumar, Computation of adsorption parameters for the removal of dye from wastewater by microwave assisted sawdust: Theoretical and experimental analysis, Environ Toxicol Pharmacol, 50, 2017, 45–57.

[30] A.S. Mestre, J. Pires, J.M.F. Nogueira, A.P. Carvalho, Activated Carbons for the Adsorption of Ibuprofen, Carbon, 45, 2007, 1979–1988.

[31] M. Heidarizad, S.S. Sengor, Synthesis of graphene oxide/magnesium oxide nanocomposites with high-rate adsorption of methylene blue, J Mol Liq, 224, 2016, 607–617.

[32] Y. Feng, D.D. Dionysiou, Y. Wu, H. Zhou, L. Xue, S. He, L. Yang, Adsorption of dyestuff from aqueous solutions through oxalic acid-modified swede rape straw: adsorption process and disposal methodology of depleted bioadsorbents, Bioresource Technol, 138, 2013, 191–197.

[33] I. Langmuir, The adsorption of gases on plane surfaces of glass, mica and platinum, J Am Chem Soc, 40, 1918, 1361–1403.

[34] G. McKay, H.S. Blair, J.R. Gardner, Adsorption of dyes on chitin. I. Equilibrium studies, J Appl Polym Sci, 27, 1982, 3043–3057.

[35] H.M.F. Freundlich, Über die adsorption in lösungen, Z Phys Chemie, 57, 1906, 385–470.

[36] L.F.M. Ismail, H.B. Sallam, S.A. Abo Farha, A.M. Gamal, G.E.A. Mahmoud, Adsorption behaviour of direct yellow 50 onto cotton fiber: Equilibrium, kinetic and thermodynamic profile, Spectrochim Acta A, 131, 2014, 657–666.

[37] M.M. Dubinin, L.V. Radushkevich, Equation of the characteristics curve of activated charcoal, Chem Zent, 1, 1947, 875.

[38] F. Helfferich, Ion Exchange, 1962, New York: McGraw-Hill.

[39] H.B. Senturk, D. Ozdes, C. Duran, Biosorption of Rhodamine 6G from aqueous solutions onto almond shell (*Prunus dulcis*) as a low cost biosorbent, Desalination, 252, 2010, 81–87.

[40] D. Balarak, J. Jaafari, G. Hassani, Y. Mahdavi, I. Tyagi, S. Agarwal, V.K. Gupta, The use of low-cost adsorbent (Canola residues) for the adsorption of methylene blue from aqueous solution: isotherm, kinetic and thermodynamic studies, Colloid Interface Sci Commun, 7, 2015, 16–19.

[41] Y. Yao, F. Xu, M. Chen, Z. Xu, Z. Zhu, Adsorption behavior of methylene blue dye on carbon nanotubes, Bioresour Technol, 101(9), 2010, 3040–3046.

[42] T.S. Natarajan, H.C. Bajaj, R.J. Tayade, Preferential adsorption behavior of methylene blue dye onto surface hydroxyl group enriched TiO2 nanotube and its photocatalytic regeneration, J Colloid Interface Sci, 433, 2014, 104–114.

[43] J. Feng, Y. Wang, L. Zou, B. Li, X. He, Y. Ren, Y. Lv, Z. Fan, Synthesis of magnetic ZnO/ZnFe2O4 by a microwave combustion method, and its high rate of adsorption of methylene blue, J Colloid Interface Sci, 438, 2015, 318–322.

[44] R. Gong, M. Li, C. Yang, Y. Sun, J. Chen, Removal of cationic dyes from aqueous solution by adsorption on peanut hull, J Hazard Mater, 121(1–3), 2005, 247–250.

[45] S. Karagoz, T. Tay, S. Ucar, M. Erdem, Activated carbons from waste biomass by sulfuric acid activation and their use on methylene blue adsorption, Bioresour Technol, 99(14), 2008, 6214–6222.

[46] S. Yao, H. Lai, Z. Shi, Biosorption of methyl blue onto tartaric acid modified wheat bran from aqueous solution, Iranian J Environ Health Sci Eng, 9(1), 2012, 16.

[47] L. Sun, D. Chen, S. Wan, Z. Yu, Performance, kinetics, and equilibrium of methylene blue adsorption on biochar derived from eucalyptus saw dust modified with citric, tartaric, and acetic acids, Bioresour Technol, 198, 2015, 300–308.

[48] G. Annadurai, R.-S. Juang, D.-J. Lee, Use of cellulose-based wastes for adsorption of dyes from aqueous solutions, J Hazard Mater, 92(3), 2002, 263–274.

[49] F.A. Batzias, D.K. Sidiras, Dye adsorption by calcium chloride treated beech sawdust in batch and fixed-bed systems, J Hazard Mater, 114(1–3), 2004, 167–174.

[50] G. Crini, H.N. Peindy, F. Gimbert, C. Robert, Removal of C.I. basic green 4 (malachite green) from aqueous solutions by adsorption using cyclodextrin-based adsorbent: Kinetic and equilibrium studies, Sep Sci Technol, 53, 2007, 97–110.

[51] Y. Ozdemir, M. Dogan, M. Alkan, Adsorption of cationic dyes from aqueous solutions by sepiolite, Micropor Mesopor Mat, 96, 2006, 419–427.

[52] N. Tekin, O. Demirbas, M. Alkan, Adsorption of cationic polyacrylamide onto kaolinite, Micropor Mesopor Mat, 85 (3), 2005, 340–350.